Hindawi Publishing Corporation
Journal of Nanomaterials
Volume 2015, Article ID 560352, 9 pages
http://dx.doi.org/10.1155/2015/560352

Research Article

Influence of Monodisperse Fe_3O_4 Nanoparticle Size on Electrical Properties of Vegetable Oil-Based Nanofluids

Bin Du, Jian Li, Feipeng Wang, Wei Yao, and Shuhan Yao

State Key Laboratory of Power Transmission Equipment & System Security and New Technology, Chongqing University, Chongqing 400044, China

Correspondence should be addressed to Jian Li; lijian@cqu.edu.cn

Received 21 January 2015; Accepted 24 May 2015

Academic Editor: Themis Matsoukas

Insulating oil modified by nanoparticles (often called nanofluids) has recently drawn considerable attention, especially concerning the improvement of electrical breakdown and thermal conductivity of the nanofluids. In this paper, three sized monodisperse Fe_3O_4 nanoparticles were prepared and subsequently dispersed into insulating vegetable oil to achieve nanofluids. The dispersion stability of nanoparticles in nanofluids was examined by natural sedimentation and zeta potential measurement. The electrical breakdown strength, space charge distribution, and several dielectric characteristics, for example, permittivity, dielectric loss, and volume resistivity of these nanofluids, were comparatively investigated. Experimental results show that the monodisperse Fe_3O_4 nanoparticles not only enhance the dielectric strength but also uniform the electric field of the nanofluids. The depth of electrical potential well of insulating vegetable oils and nanofluids were analyzed to clarify the influence of nanoparticles on electron trapping and on insulation improvement of the vegetable oil.

1. Introduction

Recent research works have shown that conductive and semiconductive nanoparticles can be dispersed in mineral and vegetable insulating oils to enhance dielectric strength or thermal conductivity of the insulating oils. Magnetic Fe_3O_4 nanoparticles have been proved of increasing the AC breakdown voltage of insulating oils for the case that the nanoparticles were well dispersed in oil [1–5]. It is also documented that both mineral and vegetable insulating oils are possible to show enhanced AC breakdown voltages and partial-discharge-inception voltages after the oils are modified by semiconductive TiO_2 nanoparticles [6, 7]. The electrical properties and dispersion stability of three nanofluids that are prepared by dispersing Fe_3O_4, TiO_2, and Al_2O_3 nanoparticles, respectively, in transformer oils have been discussed at a certain level [8]. The main process of charge transport in nanofluids is considered as the trapping and detrapping of electrons in shallow traps which has been argued in [7, 9].

It is already clarified that the dielectric performance of nanofluids is critically determined by nanoparticles' size [10, 11]. However, comparative and systematic studies on the influence of nanoparticle size on the breakdown and the dielectric properties of vegetable oil-based nanofluids are still an open issue, which is becoming more important for applying such nanofluids in large power transformers. Moreover, nanoparticles often tend to agglomerate in oil because of nanoparticle's high surface-energy. It is technically difficult to prepare sufficiently good nanoparticles (single-crystalline, well-shaped, and narrow size-distribution) for analyzing the relationship between nanoparticle size and nanofluids' dielectric responses. Recently, several models are proposed to explain the improving breakdown characteristics of nanofluids [9, 12]. However, these mechanisms are always hard to explain influence of nanoparticle size on breakdown voltages and dielectric properties of nanofluids.

Our work aims to explore how the size of monodisperse nanoparticles generates various dielectric performances of nanofluids. The insulating vegetable oil-based nanofluids were prepared by adding three sized monodisperse Fe_3O_4 nanoparticles. Their basic physical and chemical properties are first presented briefly. The dispersion stability of nanofluids was determined by comparison of zeta potential

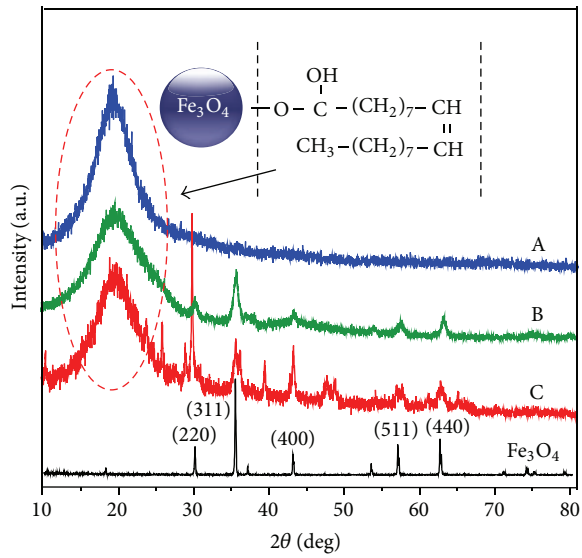

Figure 1: XRD patterns of pure Fe_3O_4 and Fe_3O_4 nanoparticle at different reaction time: (A) 12 hours, (B) 24 hours, and (C) 48 hours.

measurement. Next, the different dielectric properties of nanofluids are presented and discussed. The space charge distribution and electrical potential well depth were analyzed for the explanation of different breakdown voltages between the nanofluids and insulating vegetable oils.

2. Experimental

2.1. Materials. All reagents used in the experiment were of analytical grade without further purification.

2.2. Preparation of Nanofluids. The insulating vegetable oil-based nanofluids are obtained via three main procedures: preparation of the iron oleate precursor, preparation of the monodisperse Fe_3O_4 nanoparticle, and synthesis of the nanofluids.

2.2.1. Iron Oleate Precursor. 6.48 g of iron (III) chloride hexahydrate was dissolved in the mixture of 48 mL ethanol and 84 mL N-hexane. The obtained solution was slowly added by 21.9 g sodium-oleate-vigorous with magnetic string at 60°C for 12 h. The precipitated iron oleate was washed twice with methanol and was redissolved in hexane afterwards. The solution was additionally washed three times with warm (~60°C) deionized water in a separatory funnel and subsequently dried in vacuum at 80°C for 24 h.

2.2.2. Fe_3O_4 Nanoparticles. 2.1 g iron oleate precursor and 0.64 mL oleic acid were mixed in 10 mL octadecene followed by transferring into a three-neck-round-bottom flask and drying at 120°C for 30 min under nitrogen protection to remove water and oxygen. Then, the resulting mixture was heated to 320°C with 12 h, 24 h, and 48 h, respectively, to realize Fe_3O_4 nanoparticles with varied sizes. After cooling down to room temperature, the nanoparticles were subsequently centrifuged and washed several times with ethanol and cyclohexane before drying in air at 70°C.

Table 1: Basic physical and chemical properties of the FR3 and the insulating vegetable oil-based nanofluids.

Parameter	FR3	Nanofluids
Appearance	Light yellow	Dark yellow
Density ($kg{\cdot}m^{-3}$, 20°C)	0.90	0.90
Kinematic viscosity ($mm^2{\cdot}s^{-1}$, 40°C)	43.0	44.0
Pour point (°C)	−18	−18
Flash point (°C)	325	325
Acid value ($mg{\cdot}KOH{\cdot}g^{-1}$)	0.03	0.03
Interfacial tension (mN/m)	30	30

2.2.3. Preparation of Nanofluids. The three Fe_3O_4 nanoparticles obtained by different reaction time were dispersed in the insulating vegetable oil through ultrasonic treatment. They were tagged by samples A, B, and C, respectively. The FR3 natural ester was used as received [13]. Before electrical characterization, three nanofluids and the FR3 were dried at 85°C under 50 Pa for 72 h. Some physical and chemical parameters of the FR3 and nanofluids are listed in Table 1.

2.3. Nanoparticle Characterization. The X-ray diffraction (XRD) pattern was obtained by using a powder X-ray diffraction meter equipped with a rotating anode and a Cu-Kα radiation source. The scan step was 0.02°. Figure 1 shows the XRD results of typical Fe_3O_4 nanoparticle according to [5] and different samples were obtained by high temperature decomposition method. It can be seen from the figure that the XRD patterns of Fe_3O_4 nanoparticle near 20° have a very wide amorphous peak; this is because the nanoparticles surface

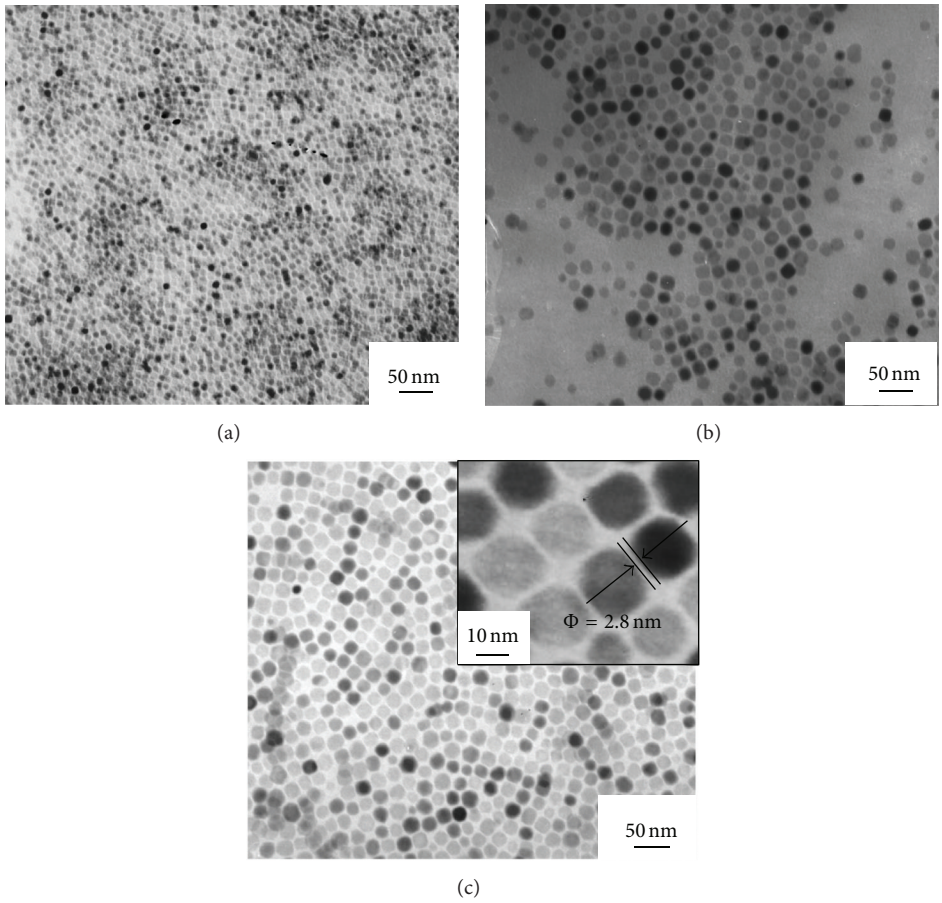

Figure 2: TEM images of monodisperse Fe_3O_4 nanoparticles at different reaction times (a) 12 hours, (b) 24 hours, and (c) 48 hours and the high resolution TEM image of monodisperse Fe_3O_4 (top right).

was coated with a large number of oleic acid. As the reaction time of sample A is not sufficient and the size is too small, there was no peak corresponding with Fe_3O_4 observed. The sharp peaks of samples B and C reveal that the nanoparticles have high crystallinity. According to JCPDS card number 65-3107, the 2θ values of 30.1°, 35.5°, 43.1°, 56.9°, and 62.6° are signatures of (220), (311), (400), (511), and (440) crystal face for Fe_3O_4, respectively. Therefore, these XRD patterns may be indicative of the spinel structure of the Fe_3O_4 nanoparticles.

The morphologies of the three sized nanoparticles were observed by transmission electron microscopy (TEM), as shown in Figure 2. It is seen that the nearly spherical Fe_3O_4 nanoparticles prepared by high temperature decomposition (at 320°C) have achieved monodispersion. Each nanoparticle consists of two differentiated contrast regions. The darker central-core is the Fe_3O_4 crystal, which is surrounded by a lower-density shell, that is, the oleic acid. The covalent bonding between oleic acid and Fe_3O_4 prevents agglomeration of Fe_3O_4 nanoparticles but also improves the compatibility between nanoparticles and vegetable insulating oil [14].

The average size of the Fe_3O_4 crystal in Figure 2(a) is estimated as ~6.6 nm. Here the size represents the diameter of Fe_3O_4 crystal without the shell. With longer reaction time, that is, from 12 to 48 h, the thickness of oleic acid shell grows slightly from ~2 to ~3 nm. Therefore sized Fe_3O_4 nanoparticles are obtained with varying diameter from ~8.6 (Figure 2(a)) to ~24.4 nm (Figure 2(c)) via ~15.2 nm (Figure 2(b)). The zoomed TEM image (inset in Figure 2(c)) better indicates the border between oleic acid shell and Fe_3O_4 crystal.

3. Results and Discussion

3.1. Dispersion Stability of Nanofluids. Natural sedimentation is an indicator of the dispersion stability for nanoparticles in nanofluids. Three sized Fe_3O_4 nanoparticles were dispersed in the vegetable oil, to realize nanofluids that are recognized as 1, 2, and 3 to examine their storage-time dependent dispersion stability. As shown in Figure 3, nanofluids show no visible agglomeration for the nanoparticles in oil after 6 months standing in ambient condition.

The zeta potential measurement is another method to evaluate stability of the nanofluids. As the stabilization theory [15] describes, the electrostatic repulsion among nanoparticles should increase prominently for the case that the zeta potential stands at a high level which signifies good suspension stability [16]. Table 2 lists several key zeta potential values that indexed the suspension stability of nanofluids.

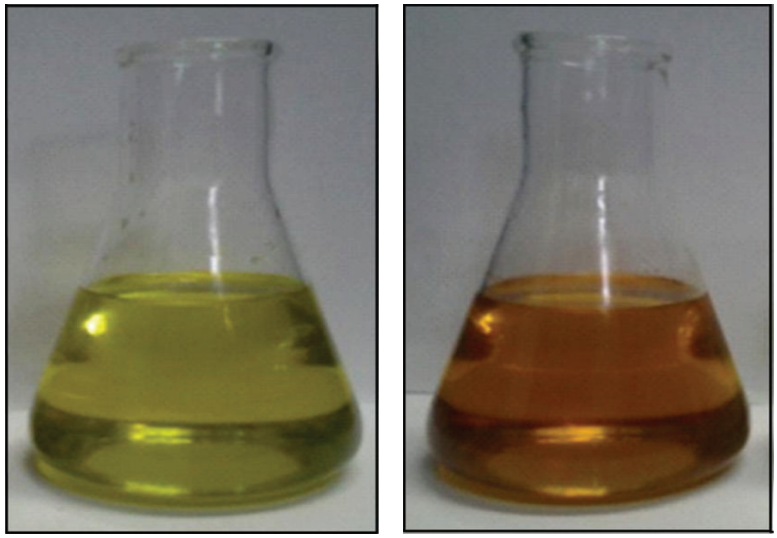

(a) (b)

Figure 3: (a) FR3 and (b) vegetable oil-based nanofluids.

Table 2: Zeta potential and associated suspension stability.

Z potential (mV)	Stability
0	Little or no stability
15	Some stability but settling lightly
30	Moderate stability
45	Good stability, possible settling
60	Very good stability, little settling likely

The zeta potential for all the three nanofluids 1, 2, and 3 display values above 30 mV, that is, 74.0, 60.7, and 47.4 mV, respectively. It has been well accepted that a zeta potential which is great than 30 mV should mark a sufficiently good dispersion stability [15]. As a general rule, the smaller nanoparticles in nanofluids, the higher the zeta potential and certainly the more stable the nanofluids.

3.2. Breakdown Voltage of Nanofluids. The absolute moisture content of all nanofluids was controlled at a value below 200 mg/kg. The AC breakdown voltages of each nanofluid were characterized in accordance with IEC 60156 [17]. All the measurements were made on 9 nanofluids samples. The FR3 oil was also included in measurements for comparison.

The lightning-impulse breakdown voltages for nanofluids were obtained by means of a configuration consisting of a container and an electrode in Figure 4. The high-voltage electrode and the grounding electrode were a steel needle and a 13 mm diametersteel sphere, respectively. The gap between the needle tip and the sphere was 15 mm. These dimensions comply with IEC 60897 [18] for liquid dielectrics. 1.2/50 μs standard lightning-impulse voltages are employed to determine the lightning-impulse breakdown voltages

Figure 5 lists the AC breakdown voltages of the three nanofluids and the FR3 oil, in which the oil was marked as

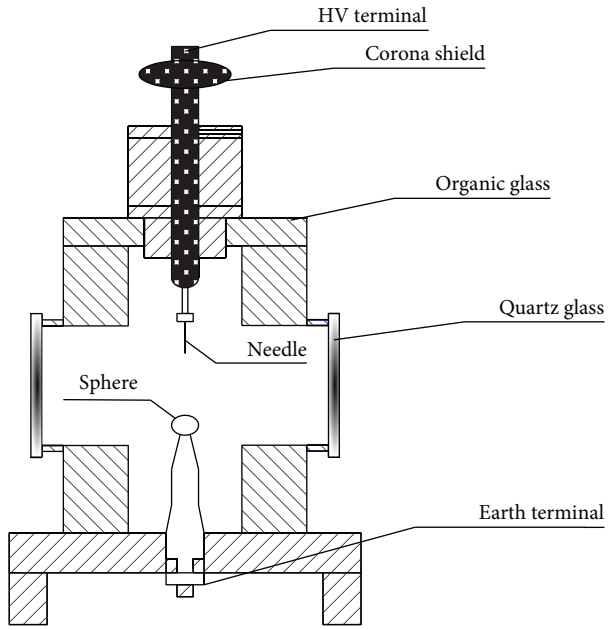

Figure 4: Sketch of electrode setup and oil vessel for lightning-impulse breakdown experiments on insulating oils.

0 ppm nanoparticles added. It is seen that the breakdown strength of each nanofluids increases to a top value and slightly decreases afterwards with higher nanoparticle content. For example, the breakdown strength enhances by 23% from 55.1 kV for FR3 to 67.8 kV for nanofluids C that was added with 200 ppm nanoparticles. On the other hand, the breakdown strength tends to increase for nanofluids with larger size nanoparticles added.

The lightning-impulse breakdown voltages of the three nanofluids and FR3 oil for both polarities are summarized in

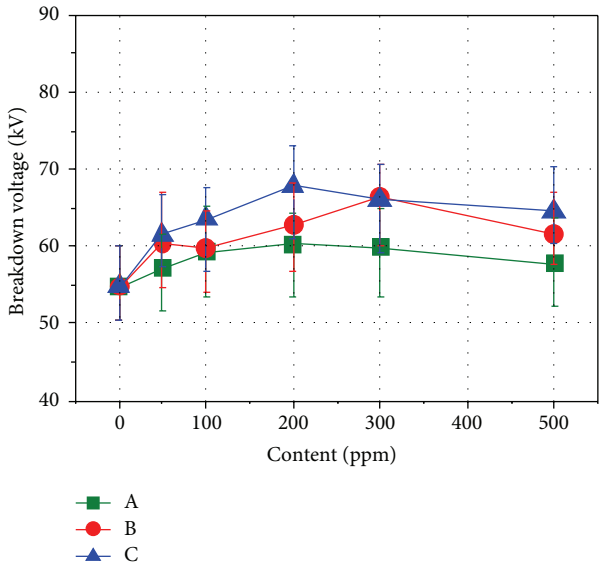

Figure 5: Influence of contents and sizes of Fe_3O_4 nanoparticles on the AC breakdown voltage of the vegetable oil-based nanofluids.

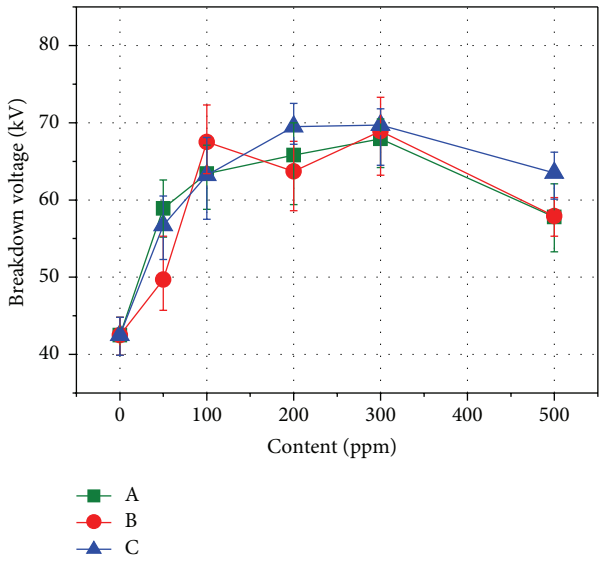

Figure 6: Influence of contents and size of nanoparticles on the positive lightning breakdown voltage of the vegetable oil-based nanofluids.

Figures 6 and 7. For negative lightning-impulse the nanofluids provide insignificant effects, but for the AC profile or for the positive lightning-impulse the attained improvement is significant. Here the positive lightning-impulse leads to strongly increased breakdown voltages. The nanofluid C, which contains 300 ppm nanoparticles, exhibits the highest breakdown voltage of 69.7 kV for positive lightning-impulse. This is a significantly higher voltage which is enhanced by 64% compared to that of FR3 oil. However the nanofluids show only slightly improved (7%) breakdown behavior for the case of negative lightning-impulse application. The increases of the positive lightning breakdown voltages are greater than

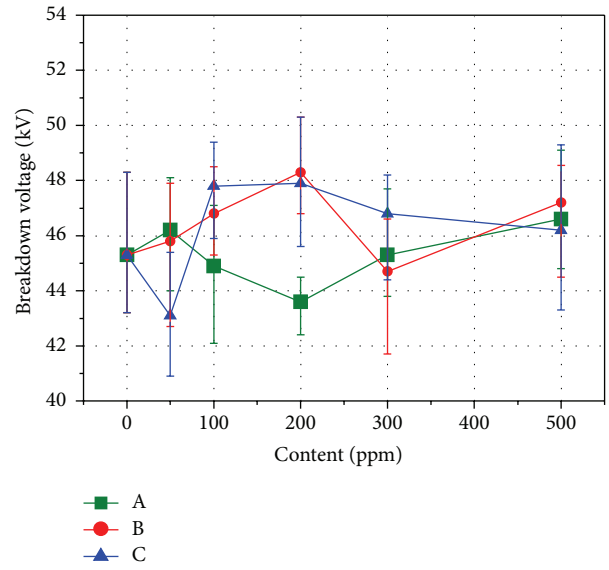

Figure 7: Influence of contents and size of nanoparticles on the negative lightning breakdown voltage of the vegetable oil-based nanofluids.

that of the negative lightning-impulse breakdown voltages. For positive lightning-impulse, nanoparticles in nanofluids will weaken the field strength and extremely increase positive breakdown voltages. However, the effect is inconspicuous for negative lightning-impulse [4]. Our results point out an opposite tendency with the breakdown behavior that has been observed in mineral oil-based nanofluids [1, 8]. This should be attributed to the much different molecular conformation of insulating vegetable oil, which certainly generates different streamer development.

From the results in Figures 5–7, one can note that the measured breakdown voltage of nanofluids follows a sequence A < B < C with nearly no influence from polarity or nanoparticle content. This encourages us to conclude that the breakdown strength of nanofluids is mainly determined by the size of nanoparticles.

3.3. Dielectric Properties of Nanofluids. The frequency dependences of permittivity between 10^{-2} and 10^6 Hz for FR3 oil and the three nanofluids are summarized in Figure 8. There is no big difference over the frequency range among samples. As well known, the relative permittivity of Fe_3O_4 nanoparticles is ca. 80 [12], which is much greater than that of FR3 oil. Therefore nanoparticles may contribute more to the permittivity of nanofluids than FR3 oil. Furthermore, at 50 Hz, the relative permittivity decreases with increasing nanoparticle size and the relative permittivity of sample A has a maximum value of 3.06.

It is obvious that the permittivity values of nanofluids varied with the size of nanoparticles. Considerable results have confirmed that smaller sized nanoparticles usually possess higher permittivity than that of larger ones. The reason can be found from an internal-stress model which has been introduced by Buessem et al. [19]; that is, the permittivity of

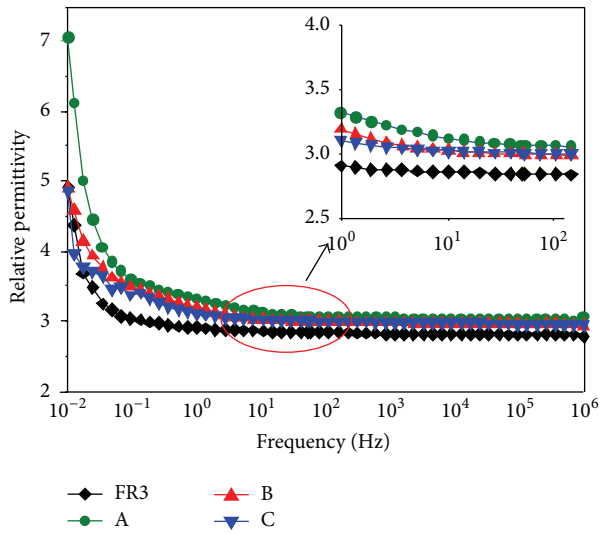

Figure 8: Variation of the relative permittivity of vegetable oil modified by Fe_3O_4 nanoparticles with different sizes at different frequencies.

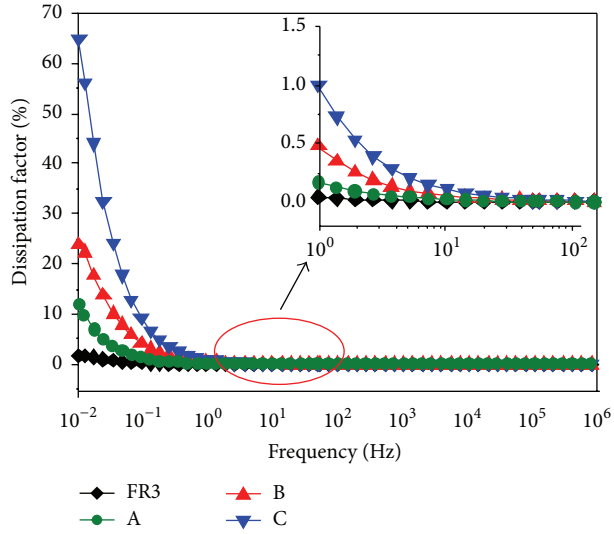

Figure 9: Variation of the dielectric loss of vegetable oil modified by Fe_3O_4 nanoparticles with different sizes at different frequencies.

a nanoparticle is determined by the relatively strong internal-stress which is the result of free-energy balance.

The dielectric loss of nanofluids and FR3 oil shows a decrease with increasing frequency as the results shown in Figure 9. However the nanofluids' loss decreases for larger sized Fe_3O_4 nanoparticles. The three nanofluids and the FR3 oil behave almost identical between 1 and 10^6 Hz. They present obvious difference at the range of 10^{-2}–1 Hz.

The loss of a fluid is composed of two contributions, that is, conductance loss and polarization loss. Vegetable insulating oil (e.g., FR3 oil in this work) is a weak polar liquid dielectric, which implies that the conductance loss dominants at low frequency [20]. The crystal defects within nanoparticles, which are unavoidable and usually are brought

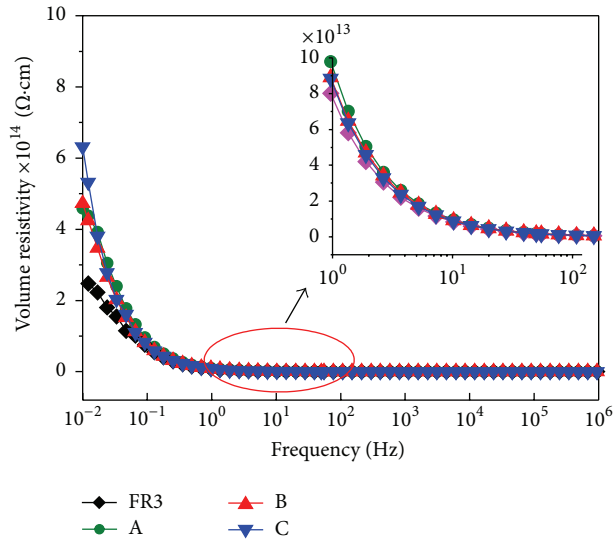

Figure 10: Variation of the volume resistivity of vegetable oil modified by Fe_3O_4 nanoparticles with different sizes at different frequencies.

during chemical preparation, emerge more for larger sized nanoparticles. The high conductivity of these nanoparticles certainly leads to much increased dielectric loss.

Figure 10 gives the frequency dependence of the volume resistivity for FR3 oil and the three nanofluids. There is no visible difference among nanofluids and FR3 oil at a frequency above 0.1 Hz. When frequency downs below 0.1 Hz, the curves start to diverge, with a changeless tendency that the volume resistivity of nanofluids is always higher than that of FR3 oil.

Nanoparticles dispersed in nanofluids are polarized when the nanofluids are subjected to an externally applied electric field [12]. These nanoparticles provide traps free electrons, thereby decreasing the concentration of highly mobile electrons in the nanofluids and increasing the concentration of low-mobility negatively charged nanoparticles. As a result, the volume resistivity of the nanofluids is larger than that of the vegetable insulating oil. Increasing the frequency decreases both the duration of each half cycle of the electrical field and the probability of electron capture by the nanoparticles. These phenomena explain the smaller difference in volume resistivity between the FR3 oil and the nanofluids at frequencies greater than approximately 0.1 Hz.

3.4. Space Charge Distribution of Nanofluids. In order to investigate the influence of sizes of monodisperse Fe_3O_4 nanoparticle on charge carriers transport characteristics of the vegetable oil and vegetable oil-based nanofluids, the pulse electroacoustic (PEA) tests were carried out to investigate the space charge density of all samples, stressed 15 kV/mm for varying time (0.5, 1, 5, 10, and 30 min). As shown in Figure 11, the charge density in vegetable oil is increasing with time and the maximum charge density was about 34.2 C/m^3. However, the charge density in nanofluids was first increased and then decreased with time, less than half of that in vegetable oil. The

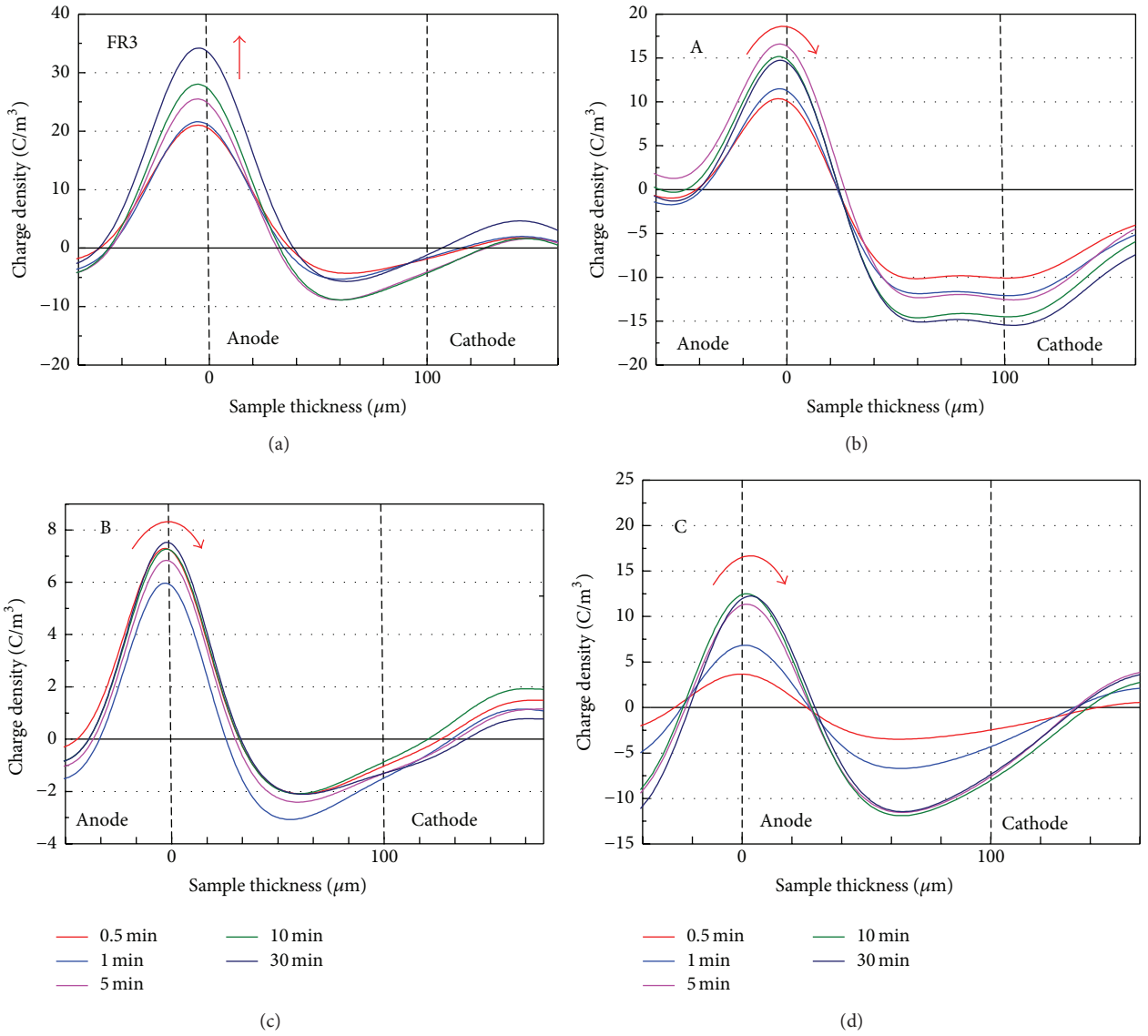

FIGURE 11: Charge density of the samples vegetable oil modified by Fe_3O_4 nanoparticles with different sizes.

maximum charge density of the three nanofluids was about 16.6, 12.5, and 7.5 C/m^3, respectively.

The similar results also can be found in [7, 21, 22]. Interaction between nanoparticles and vegetable oil molecule will significantly improve the charge mobility of nanofluids. And the rapid charge mobility may inhibit space charge accumulation, resulting in uniform electric field of nanofluids.

3.5. Possible Mechanism. To understand why the breakdown voltage of nanomodified insulating vegetable oil is higher than that of pure vegetable oil, a dipole model of nanoparticles in [23] is proposed. The charge relaxation time constant of nanoparticles has a major bearing on the extent to which the electrodynamics processes in the liquid are modified. If the nanoparticles' charge relaxation time constant is short, then the timescales of interest for streamer growth and their presence in the oil will significantly modify the electrodynamics.

The spherical nanoparticles (diameter $2a$, relative dielectric constant ε_2) were dispersed in the insulating oils (relative dielectric constant ε_1) as shown in Figure 12, and an external electric field E_0 was applied to the vegetable oil-based nanofluids consisting of ε_1 and ε_2 dielectrics. According to the calculation, the relaxation time constant of the nanoparticle Fe_3O_4 used in the test is less than the propagation time of the streamer [4]. Electric charges will be induced by the electric field E_0 at the surface of the spherical body. As a result, the dipole surface charge density, $\sigma_p(\theta_p, \varphi_p)$, given by (1), is induced by the applied electric field E_0 at the interface between the ε_1 and ε_2 dielectrics:

$$\delta_p = \varepsilon_0 E_0 \left(1 - \frac{3\varepsilon_1}{2\varepsilon_1 + \varepsilon_2}\right) \cos\varphi_p \sin\theta_p. \quad (1)$$

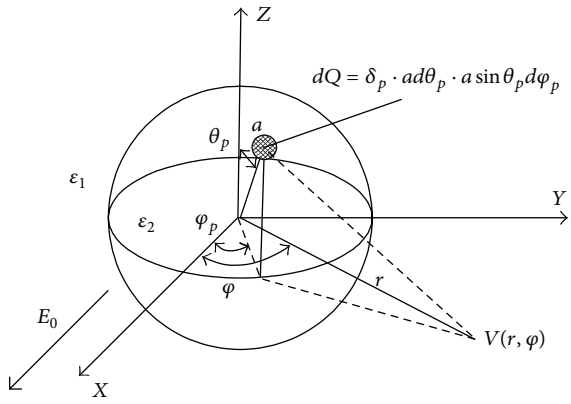

Figure 12: Diagram depicting the dipole surface charge density, $\sigma_p(\theta_p, \varphi_p)$, and the electrical potential, $V(r, \varphi)$, in spherical coordinates.

As the direction of E_0 was set in the direction of the x-axis, angle $\varphi = 0$, the positive dipole surface charge, $+\sigma_p(\theta_p, \varphi_p)$, was induced within the angle range $-\pi/2 < \varphi_p < +\pi/2$, and the negative dipole surface charge, $-\sigma_p(\theta_p, \varphi_p)$, was induced within the angle range $\pi/2 < \varphi_p < 3\pi/2$. The electrical potential distribution, $V(r, \varphi)$, induced by the dipole surface charge density, $\sigma_p(\theta_p, \varphi_p)$, expressed as (1), is given by (2). Equation (2) is normalized by the potential difference aE_0:

$$V(r, \varphi) = \frac{aE_0}{4\pi}\left(1 - \frac{3\varepsilon_1}{2\varepsilon_1 + \varepsilon_2}\right) \cdot \int_{-\pi}^{+\pi}\int_{0}^{+\pi} \frac{\sin^2\theta_p d\theta_p \cos_p d\varphi_p}{\sqrt{1 + (r/a)^2 - 2(r/a)\sin\theta_p \cos(\varphi - \varphi_p)}}. \quad (2)$$

Figure 13 showed the electrical potential well distribution, $V(r)$, at $\varphi = 0$ which was obtained from (2). The size of nanoparticle was $a = 10$, 20 and 30 nm, respectively, and the external electric field is $E_0 = 200$ kV/mm. Furthermore, the relative dielectric constant of the Fe_3O_4 nanoparticle was $\varepsilon_1 = 80$ and vegetable insulating oil was $\varepsilon_2 = 3.2$.

In Figure 13, it can be seen that the maximum electrical potential well occurred at the surface of the nanoparticle. The maximum electrical well of nanoparticle grows linearly with increasing the nanoparticle size. When the nanoparticle size was 10 nm, 20 nm, and 30 nm, the maximum electrical potential well depth was 5.86, 11.73, and 17.59 eV, respectively. The electrical potential well depth was much higher than that of insulating oil (about 0.45 eV) [23]. The increased electrical potential well depth in nanofluids could inhibit the free charge spread and enhance the capability of breakdown performance of nanofluids.

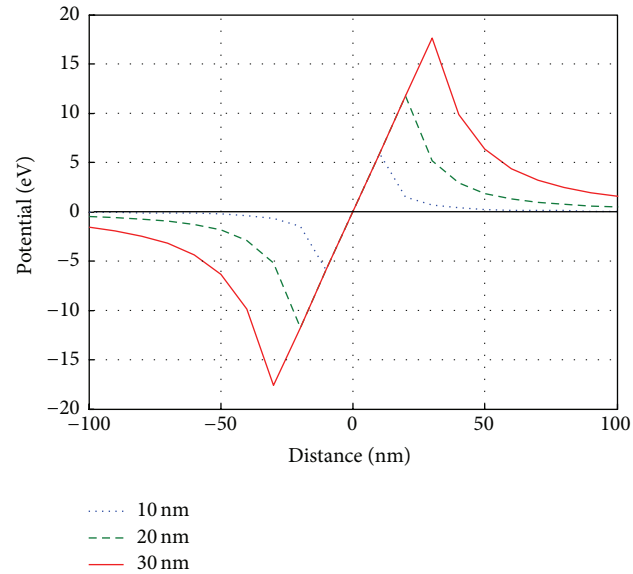

Figure 13: Dependence on size of nanoparticle induced trapped depth.

4. Conclusion

(1) The nanofluids were developed by dispersing Fe_3O_4 nanoparticles with different sizes in insulating vegetable oil to enhance its breakdown strength. For negative lightning-impulse the nanofluids provide insignificant effects, but for the AC profile or for the positive lightning-impulse the attained improvement is significant. Meanwhile, the increasing nanoparticle size will improve the breakdown performance of nanofluids.

(2) With increasing the nanoparticle size, the volume resistivities of the nanofluids are almost equal and their dissipation factors increase at frequencies below 0.1 Hz. The relative permittivities of the nanofluids are greater than that of the FR3 oil between 10^{-2} and 10^7 Hz, probably because of the much higher relative permittivity of the Fe_3O_4 nanoparticles.

(3) The addition of monodisperse Fe_3O_4 nanoparticle into vegetable insulating oil will increase the electrical potential well depth and nanoparticle size could significantly influence the electrical potential well depth. The increased electrical potential well depth could enhance the capability of breakdown performance of nanofluids.

Conflict of Interests

The authors declare that they have no financial or personal relationship with any people or any organization that may inappropriately influence their work and there is no professional or commercial interest of any kind in all of the commercial entities mentioned in our paper.

Acknowledgments

The authors acknowledge the National Science Foundation of China (nos. 51321063 and 51377176) and the 111 Project of the Ministry of Education, China (B08036). A visiting scholarship provided by the State Key Lab of Power Equipment &

System Security and New Technology at Chongqing University (no. 2007DA10512713408) and the Doctoral Program of Higher Education of China (SRFDP) (20110191110017) are also appreciated for supporting this work.

References

[1] J. A. Mergos, M. D. Athanassopoulou, T. G. Argyropoulos, and C. T. Dervos, "Dielectric properties of nanopowder dispersions in paraffin oil," *IEEE Transactions on Dielectrics and Electrical Insulation*, vol. 19, no. 5, pp. 1502–1507, 2012.

[2] V. Segal, A. Rabinovich, D. Nattrass, K. Raj, and A. Nunes, "Experimental study of magnetic colloidal fluids behavior in power transformers," *Journal of Magnetism and Magnetic Materials*, vol. 215, pp. 513–515, 2000.

[3] P. Zou, J. Li, C. Sun, Z. Zhang, and R. Liao, "Dielectric properties and electrodynamic process of natural ester-based insulating nanofluid," *Modern Physics Letters B*, vol. 25, p. 2021, 2011.

[4] J. Li, Z. Zhang, P. Zou, B. Du, and R. Liao, "Lightning impulse breakdown characteristics and electrodynamic process of insulating vegetable oil-based nanofluid," *Modern Physics Letters B*, vol. 26, no. 15, Article ID 1250095, 13 pages, 2012.

[5] J. Li, Z. Zhang, P. Zou, S. Grzybowski, and M. Zahn, "Preparation of a vegetable oil-based nanofluid and investigation of its breakdown and dielectric properties," *IEEE Electrical Insulation Magazine*, vol. 28, no. 5, pp. 43–50, 2012.

[6] D. Yue-Fan, L. Yu-Zhen, L. Cheng-Rong et al., "Effect of electron shallow trap on breakdown performance of transformer oil-based nanofluids," *Journal of Applied Physics*, vol. 110, p. 104, 2011.

[7] Y.-F. Du, Y.-Z. Lv, C. Li et al., "Effect of semiconductive nanoparticles on insulating performances of transformer oil," *IEEE Transactions on Dielectrics and Electrical Insulation*, vol. 19, no. 3, pp. 770–776, 2012.

[8] W.-X. Sima, X.-F. Cao, Q. Yang, H. Song, and J. Shi, "Preparation of three transformer oil-based nanofluids and comparison of their impulse breakdown characteristics," *Nanoscience and Nanotechnology Letters*, vol. 6, no. 3, pp. 250–256, 2014.

[9] Y.-X. Zhong, Y.-Z. Lv, C.-R. Li et al., "Insulating properties and charge characteristics of natural ester fluid modified by TiO_2 semiconductive nanoparticles," *IEEE Transactions on Dielectrics and Electrical Insulation*, vol. 19, pp. 770–776, 2012.

[10] P. Kopčanský, L. Tomcčo, K. Marton, M. Koneracká, M. Timkoa, and I. Potočová, "The DC dielectric breakdown strength of magnetic fluids based on transformer oil," *Journal of Magnetism and Magnetic Materials*, vol. 289, pp. 415–418, 2005.

[11] J.-C. Lee, W.-H. Lee, S.-H. Lee, and S. Lee, "Positive and negative effects of dielectric breakdown in transformer oil based magnetic fluids," *Materials Research Bulletin*, vol. 47, no. 10, pp. 2984–2987, 2012.

[12] J. G. Hwang, M. Zahn, F. M. O'Sullivan, L. A. A. Pettersson, O. Hjortstam, and R. Liu, "Effects of nanoparticle charging on streamer development in transformer oil-based nanofluids," *Journal of Applied Physics*, vol. 107, no. 1, Article ID 014310, 2010.

[13] Q. Liu and Z. D. Wang, "Streamer characteristic and breakdown in synthetic and natural ester transformer liquids under standard lightning impulse voltage," *IEEE Transactions on Dielectrics and Electrical Insulation*, vol. 18, no. 1, pp. 285–294, 2011.

[14] Y. Ren, K.-I. Iimura, and T. Kato, "Structure of barium stearate films at the air/water interface investigated by polarization modulation infrared spectroscopy and π – A isotherms," *Langmuir*, vol. 17, no. 9, pp. 2688–2693, 2001.

[15] J.-H. Lee, K. S. Hwang, S. P. Jang et al., "Effective viscosities and thermal conductivities of aqueous nanofluids containing low volume concentrations of Al_2O_3 nanoparticles," *International Journal of Heat and Mass Transfer*, vol. 51, no. 11-12, pp. 2651–2656, 2008.

[16] L. Vandsburger, *Synthesis and Covalent Surface Modification of Carbon Nanotubes for Preparation of Stabilized Nanofluid Suspensions*, Department of Chemical Engineering, McGill University, Montreal, Canada, 2009.

[17] Insulating Liquids—Determination of the Breakdown Voltage at Power Frequency—Test Method, IEC 60156, 1995.

[18] Methods for the determination of the lightning impulse breakdown voltage of insulating liquids, IEC 60897, 1987.

[19] W. Buessem, L. Cross, and A. Goswami, "Phenomenological theory of high permittivity in fine-grained barium titanate," *Journal of the American Ceramic Society*, vol. 49, no. 1, pp. 33–36, 1966.

[20] R. Richert, A. Agapov, and A. P. Sokolov, "Appearance of a Debye process at the conductivity relaxation frequency of a viscous liquid," *The Journal of Chemical Physics*, vol. 134, no. 10, Article ID 104508, 2011.

[21] J. K. Nelson and J. C. Fothergill, "Internal charge behaviour of nanocomposites," *Nanotechnology*, vol. 15, no. 5, pp. 586–595, 2004.

[22] T. Tanaka, "Dielectric nanocomposites with insulating properties," *IEEE Transactions on Dielectrics and Electrical Insulation*, vol. 12, no. 5, pp. 914–928, 2005.

[23] T. Takada, Y. Hayase, and Y. Tanaka, "Space charge trapping in electrical potential well caused by permanent and induced dipoles for LDPE/MgO nanocomposite," *IEEE Transactions on Dielectrics and Electrical Insulation*, vol. 15, no. 1, pp. 152–160, 2008.